Journal of Engineering in Industrial Research

2026, Volume 7, Issue 3

Review Article

Iron Oxide–Incorporated Graphene–TiO_2 Multifunctional Nanostructures for High-Efficiency Dye-Sensitized Solar Cells: A Review

Kayode John Olaniyi[1], Sodiq Areo Akintoyese[1], Mayowa James Johnson[1,2], Joseph Olumide Ajiboye[1], Olufunke Lydia Adedeji[3], Gabriel Ayinde Alamu[1], Mojoyinola Kofoworola Awodele[1,4], Yekinni Kolawole Sanusi[1,4], Oluwaseun Adedokun[1,4,*]

[1]*Department of Pure and Applied Physics, Ladoke Akintola University of Technology, Ogbomoso, Nigeria*
[2]*Department of Physics and Materials Science, Kwara State University, Malete, Nigeria*
[3]*Department of Chemical Science, Yaba College of Technology, Yaba, Nigeria*
[4]*Nanotechnology Research Group (NANO+), Ladoke Akintola University of Technology, Ogbomoso, Nigeria*

Citation K.J. Olaniyi, S.A. Akintoyese, M.J. Johnson, J.O. Ajiboye, O.L. Adedeji, G.A. Alamu, M.K. Awodele, Y.K. Sanusi, O. Adedokun. Iron Oxide–Incorporated Graphene–TiO_2 Multifunctional Nanostructures for High-Efficiency Dye-Sensitized Solar Cells: A Review. *J. Eng. Ind. Res.* **2026**, 7(3):144-167.

https://doi.org/10.48309/jeires.2026.553353.1319

Article info:
Submitted: 2025-10-14
Revised: 2025-12-19
Accepted: 2026-01-04
ID: JEIRES-2510-1319

Keywords:
Dye-sensitized solar cells; Photoanode; Nanocomposite; High-efficiency; Multifunctional

ABSTRACT

Dye-sensitized solar cells (DSSCs) have emerged as a promising renewable energy technology over the past two decades; yet, their widespread application is hindered by issues of efficiency and stability. As the primary electron transport medium, the photoanode is a critical component that dictates the overall power conversion efficiency (PCE) of a DSSC. To overcome the limitations of conventional titanium dioxide (TiO_2) photoanodes, researchers have explored incorporating various nanostructures. This review highlights recent advancements in using iron oxide-graphene-TiO_2 nanocomposites as a multifunctional photoanode materials. It explores the synergistic effects among the components: iron oxide extends the photoanode's light absorption into the visible spectrum, graphene enhances electron transport, and TiO_2 provides structural integrity and primary photoactivity. Various synthesis and characterization techniques are reviewed, which were used to create these composites and discuss their direct impact on the composites' properties and performance. Despite significant progress, challenges remain in optimizing synthesis strategies, improving scalability, and ensuring long-term stability. Ultimately, this review demonstrates the immense potential of iron oxide-graphene-TiO_2 nanocomposites for creating high-efficiency DSSCs, highlighting both their promise and the key challenges that must be addressed for future development.

***Corresponding Author: Oluwaseun Adedokun** (oadedokun@lautech.edu.ng)*

Introduction

In the world today, the rising energy demands due to the ever-increasing human population and the gradual depletion of conventional fossil fuels has made transition toward sustainable and renewable energy sources a matter of importance. There are various types of renewable energy such as thermal energy, geothermal energy, solar energy, wind energy, etc. Among the various renewable energy sources, solar energy offers abundant, sustainable and eco-friendly power that has enormous potential for meeting global energy consumption demands because the sun which is the primary source of solar energy is readily available and accessible to everyone [1].

There have been several evolutions of solar cells, which range from the first generation (silicon solar cells) to second generation (thin-film solar cells) and to the present third generation. Silicon-based p–n solar cells, which include monocrystalline and polycrystalline silicon cells, are the first generation solar cells, that have high efficiency but are expensive to manufacture for reasons such as the very high temperature (over 1,600 °C) required to obtain silicon by reducing silica. To overcome the high-cost issue for silicon solar cells, thin-film solar cells with low cost (second-generation solar cells) were developed using inexpensive amorphous silicon and other semiconducting materials like copper indium gallium selenide (CIGS), cadmium telluride (CdTe), and gallium arsenide (GaAs) [2]; however, the efficiency of the second generation solar cells is relatively low compared with the silicon cells. The third generation solar cells such as dye sensitized solar cells, perovskite solar cells, quantum dot sensitized solar cells, have therefore been explored with the aim of achieving both low cost and relatively high efficiency. Dye-sensitized solar cells (DSSCs) are a type of third generation photovoltaic technology that offers a promising alternative to traditional silicon-based solar cells and the second generation thin-film solar cells due to their low-cost materials, simple manufacturing processes, and aesthetic versatility [3,4]. DSSC was first developed in the early 1990s by Michael Grätzel and Brian O'Regan; it mimics natural photosynthesis using a dye molecule to absorb sunlight and generate electrical energy. The basic components of a DSSC include a photoanode (typically made of a mesoporous titanium dioxide film coated with a light-absorbing dye), an electrolyte containing a redox couple, and a counter electrode [5,6]. When sunlight strikes the dye, electrons are excited and injected into the conduction band of the TiO_2, causing current to flow through the external circuit [7–9]. Although DSSCs typically offer lower efficiencies compared to conventional silicon cells, their potential for use in flexible, lightweight, and semi-transparent applications makes them attractive for integration into building materials, portable devices, and indoor energy harvesting [6,8,10,11].

The photoanode in DSSCs plays a crucial role in supporting dye molecules that absorb sunlight and excite photoelectrons [7,12–14]. The commonly used material for the photoanode in DSSCs is titanium dioxide (TiO_2) which is non-toxic, environmentally friendly, low cost and stable. Despite the potential of DSSCs, they have several notable limitations that restrict their broader application. One of the primary drawbacks is their relatively low power conversion efficiency compared to traditional silicon-based solar cells. The conversion efficiency of TiO_2 nanoparticle-based DSSCs is limited by the slow transportation of electrons through the randomly arranged nanoparticles as well as the energy losses caused by the recombination [4, 15–17]. While silicon cells can exceed 20% efficiency, DSSCs typically operate in the range of 7–11% under standard sunlight, limiting their effectiveness for high-energy-demand applications [6,9,18,19]. To overcome these limitations, band-gap engineering of TiO_2 through doping with non-metals, metals, and metal oxides has been widely explored [8,16,20]. In addition, integrating nanostructures such as nanorods, carbon nanotubes, nanowires, and graphene with TiO_2 nanoparticles has been shown to significantly enhance charge transport and overall device performance [21–23].

Nanoscience and nanotechnology have enabled the development of hybrid and multifunctional materials for harnessing solar energy [8,22]. Hybrid nanomaterials consist of more than two

nanomaterials to improve the individual performance of the components [24]. These materials hold great promise for advancing the capabilities of solar technologies by enhancing energy conversion and harvesting devices. Graphene is a single-atom-thick planar sheet of hexagonally arrayed sp2 carbon atoms has attracted significant interest in the last decade in materials science and energy related research. In particular, graphene has garnered considerable attention for the development of photoanode of DSSCs. The incorporation of graphene into DSSC photoanodes induces lower recombination, increased electron transport kinetics, enhanced light scattering effects, and concurrently boosts the power conversion efficiency (PCE) [11,25,26]. Research has been carried out over the years on the incorporation of graphene into TiO_2 and other metal oxide semiconductor based DSSCs [14,25,27,28]. In all cases, the graphene-incorporated DSSC showed improved PCE [4].

Iron oxide is a metal mixture with several crystal arrangements capable of modifying structural and magnetic properties of various nanostructures. Magnetite (Fe_3O_4), hematite (-Fe_2O_3), and maghemite (-Fe_2O_3) are the most typical forms of these metals [29]. The incorporation of iron oxide nanoparticles (Fe_2O_3) into the graphene–TiO_2 composite introduces additional functional advantages. Iron oxide serves as a light-scattering agent, improves catalytic activity, and facilitates faster electron injection and transport [30,31]. The synergistic effect of combining graphene, iron oxide, and TiO_2 leads to the formation of multifunctional nanostructures that have the potential to significantly enhance the efficiency and performance of DSSCs [32].

In recent times, research has been carried out on iron oxide-graphene-TiO_2 nanocomposites for various applications such photocatalytic degradation, water splitting and air purification. It has been reported that the incorporation of iron oxide and graphene materials into pristine TiO_2 enhances the photocatalytic properties of the parent material [33,34]. Although limited work has been reported using the combination of these three components as photoanodes in DSSCs but the unique properties of the individual components show that there will be a synergistic interaction between them if combined, thus having the potential to be an efficient photoanode material in DSSCs. This review highlights the recent developments and contributions of works that have been carried out on the engineering of advanced nanostructures by the incorporation of graphene and iron oxide into TiO_2 photoanode materials for efficient DSSCs.

Photoanodes in DSSCs

The photoanode serves as the overall energy conversion center and, thus having a critical role in the DSSC. The photoanode is made up of three essential components: a conducting substrate, a layer of semiconducting material, and sensitizers, as shown in Figure 1. The semiconducting material usually a wide bandgap metal oxide, is deposited on the surface of transparent conducting oxide (TCO) substrate, typically fluorine doped tin oxide (FTO) glass. The functions of TCO substrate in DSSC are to support the semiconductor layer and to collect the current. An ideal TCO substrate should possess high optical transparency and low electrical resistivity [7,35]. High transparency is essential to allow the good transmittance of sunlight through the substrate without unwanted adsorption, while low resistivity is crucial in facilitating the charge transfer process and reducing the energy loss. FTO is the most widely used oxide in DSSC applications due to its excellent electrical conductivity and optical transparency. Wide bandgap metal oxide semiconductors (Eg > 3 eV), such as TiO_2, ZnO, SnO_2, and Nb_2O_5 have been commonly used as photoanode materials due to their good stability against photocorrosion (transparent to the major part of the solar spectrum) and favorable electronic properties [3,7,21,36,37].

Titanium dioxide

TiO_2 is the most widely used photoanode material in dye-sensitized solar cells (DSSCs) due to its excellent chemical stability, non-toxicity, low cost, and environmental friendliness.

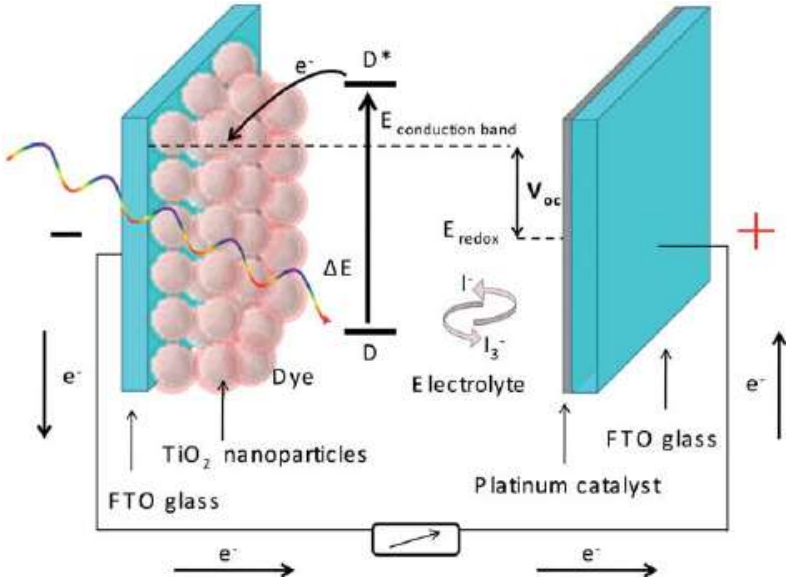

Figure 1: A schematic representation of a DSSC [38]

These properties make it highly suitable for long-term operation and large-scale applications in solar energy devices. The high surface area of nanostructured TiO_2 enables effective dye loading, which enhances light absorption and photon harvesting [39]. In addition, its wide bandgap (~3.2 eV) provides good transparency in the visible region and supports efficient electron injection from the excited dye molecules. Furthermore, TiO_2 exhibits favorable energy band alignment with commonly used dyes and electrolytes, promoting efficient charge separation and collection. Its well-established synthesis and fabrication methods also allow easy modification through doping and nanostructuring to improve electron transport and reduce recombination losses [3,35]. Besides, TiO_2 has higher CB edge, electron affinity, dye loading and surface area compared with other transition metal oxides, which makes it the most suitable choice as photoanode for DSSC applications [38]. Titanium dioxide exists in three primary crystalline forms, namely anatase (tetragonal), brookite (orthorhombic) and rutile (tetragonal) as shown in Figure 2 [14,40]. These phases of TiO_2 have their respective properties as described in Table 1. Rutile is the most stable form thermodynamically. However, anatase is more preferred in DSSC applications due to its better efficiency for solar energy conversion and photocatalysis [1,41]. Zhang *et al.* [42] reported that, anatase belongs to the indirect bandgap semiconductor category, while rutile and brookite are direct bandgap semiconductors [43]. Due to the indirect bandgap of anatase, it is impossible for photoexcited electrons to undergo direct transitions from conduction band (CB) to valence band (VB) of anatase. As a consequence, the lifetime of photoexcited electrons is longer in anatase compared with rutile and brookite. Besides, the average effective mass of photoexcited electrons in anatase is also the lightest among the three polymorphs. This allows faster migration of photoexcited electrons and hence lower recombination rate in anatase compared with rutile and brookite [21]. Park *et al.* reported that anatase-based cell has higher short-circuit photocurrent (Jsc) than rutile-based cell, while the open-circuit voltage (Voc) is the same for both cases [44]. In the recent years, a wide variety of TiO_2 nanostructures have been synthesized as photoanodes for DSSC applications such as nanoparticles, nanorods, nanowires, nanotubes and nanosheets [1,5,9,22,45]. Several fabrication methods such as sol gel, hydrothermal, spray pyrolysis, electrochemical deposition, spin coating, and chemical vapor deposition have been reported for the synthesis of various TiO_2 architectures [46–48].

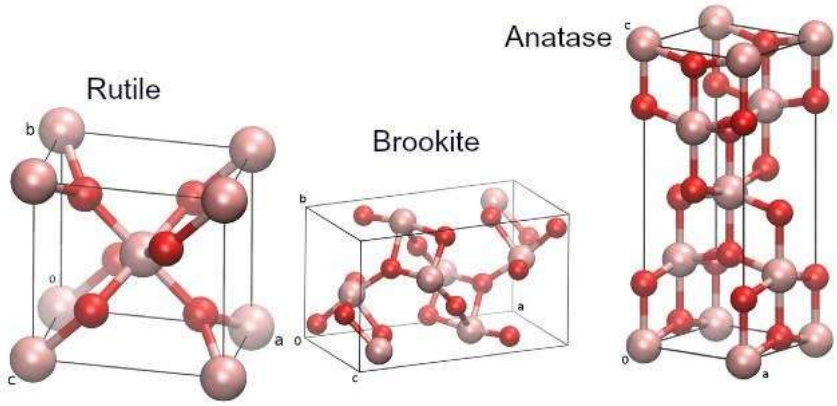

Figure 2: Crystalline phases of TiO_2 [49]

Table 1: Properties of TiO_2 [50]

Property	Anatase	Rutile	Brookite
Crystal structure	Tetragonal	Tetragonal	Orthorhombic
Lattice constant (A°)	a=3.79, c=9.51	a=4.59, c=2.96	a=9.17, b=5.46, and c=5.14
Density (g cm^{-3})	3.79	4.13	3.99
Refractive index	2.561, 2.488	2.605–2.616, 2.890–2.903	2.583, 2.700
Bandgap (eV)	3.2±0.1	3.0±0.1	3.4±0.1
Light absorption (nm)	<390	<415	300 – 400
Bulk conductivity (Scm^{-1})	5×10^{-8}	10^{-2}–10^{-7}	3×10^{-7}

The Multifaceted Contributions of Graphene in TiO_2 Photoanodes

Graphene, a two-dimensional sheet of sp^2-hybridized carbon atoms, has emerged as a powerful additive in semiconductor-based photoanodes due to its exceptional electrical, structural, and surface properties. When integrated with TiO_2 in DSSCs, graphene enhances the functionality of the photoanode in several key ways. Its unique attributes contribute to improved charge transport, light harvesting, and material morphology, making it a valuable component for optimizing DSSC performance [26,27,50].

Graphene outstanding electrical conductivity (up to 10^6 S/m) plays a crucial role in facilitating fast electron transport from the excited dye molecules through the TiO_2 matrix to the collecting electrode. When incorporated into TiO_2, graphene acts as a conductive bridge or electron highway, accelerating the transfer of photogenerated electrons and significantly reducing electron recombination with the oxidized dye or electrolyte species [17,27,51]. This improvement leads to a longer electron lifetime, higher photocurrent density, and ultimately, enhanced power conversion efficiency in DSSCs (Table 2). Another vital contribution of graphene in the TiO_2 photoanode is its high specific surface area (~2600 m^2/g), which, when combined with TiO_2 nanoparticles, increases the active surface available for dye loading [52,53]. Enhanced dye adsorption results in greater light absorption, leading to more efficient photon-to-electron conversion. The larger surface area provided by the graphene-TiO_2 network allows for better interaction between the photoanode and the dye molecules, thereby boosting the overall photoresponse of the solar cell [4,54].

The intimate contact between graphene and TiO_2 forms a favorable heterojunction, which enhances interfacial electron transfer from the excited dye to the conduction band of TiO_2 and subsequently to graphene. This synergistic interface minimizes potential energy barriers and enhances electron injection efficiency, thus

accelerating the charge separation process [55]. The improved interfacial connection also stabilizes the photoanode architecture, reducing energy losses associated with poor connectivity or charge trapping [17]. Graphene incorporation significantly influences the morphology and porosity of the TiO_2 film. Graphene sheets act as spacers that prevent the agglomeration of TiO_2 nanoparticles, resulting in a more uniform and porous structure. Increased porosity facilitates better electrolyte penetration and ionic mobility within the photoanode, while uniform dispersion enhances light absorption and charge transport pathways. This structural improvement ensures a more stable and efficient photoanode configuration [53,56]. Although graphene is not a strong light-scattering material on its own, when it interacts with iron oxide nanoparticles and TiO_2, it can create composite structures that improve internal light scattering. When embedded within TiO_2 films, graphene-based materials can alter the optical path length of incident light, allowing more photons to be absorbed by the dye. This indirect enhancement contributes to more effective light harvesting, increasing the number of photogenerated electrons and boosting the overall efficiency of the DSSC [57].

Table 2: Photovoltaic performances of DSSC with and without the incorporation of graphene/graphene composite interfacial layers

Photo electrodes	Jsc (A/m^2)	Voc (V)	FF (%)	PCE (%)	Ref.
TiO_2	81	0.68	51.8	2.9	[58]
GO/TiO_2	87	0.69	53.8	3.2	
TiO_2	111	0.74	0.66	5.7	[59]
rGO/TiO_2	150	0.74	0.66	57.5	
TiO_2	62	0.70	0.61	2.7	[27]
rGO/TiO_2	104	0.71	0.67	4.95	
TiO_2	136	0.73	0.71	7.13	[60]
TiO_2/GO	138	0.74	0.71	7.35	

The Diverse Roles of Iron Oxide in Graphene–TiO_2 Composites

Iron oxide nanoparticles, particularly in the forms of α-Fe_2O_3 (hematite), γ-Fe_2O_3 (maghemite), and Fe_3O_4 (magnetite), have emerged as multifunctional materials with promising applications in photovoltaics. When incorporated into graphene–TiO_2 composites, they serve photoactive, catalytic, electronic, and magnetic functions, each contributing to the improved performance of DSSCs. Diverse optical, electronic, and surface properties allow them to enhance light absorption, facilitate charge transport, and suppress recombination, making them an integral component of the hybrid photoanode system [61].

Iron oxides possess narrow band gaps compared to TiO_2, enabling them to absorb visible light more effectively [29]. α-Fe_2O_3 (hematite) has a bandgap of approximately 2.1 eV and can absorb light up to approximately 590 nm. γ-Fe_2O_3 (maghemite) shows similar light absorption in the visible region, with strong photon absorption up to approximately 550–600 nm. Fe_3O_4 (magnetite), with a bandgap of 2.85 eV, absorbs broadly in the visible to near-infrared region [62,63]. By incorporating these iron oxide phases into TiO_2-based photoanode, the light absorption range is extended well beyond TiO_2's UV limitation (~3.2 eV, 388 nm), allowing the photoanode to utilize a broader portion of the solar spectrum[30].

Broadening the spectral response of the photoanode

The presence of iron oxide nanoparticles contributes to spectral broadening by introducing additional light-absorbing centers within the composite. These centers enable the dye-sensitized system to better harvest photons in the visible light range, effectively increasing the photocurrent generation under sunlight. When combined with graphene and TiO_2, iron oxides support complementary absorption,

leading to improved spectral overlap with sunlight and enhanced solar-to-electric energy conversion efficiency [31,50].

Improved electron injection and transport

Iron oxides have conduction band edges that can align favorably with those of TiO_2 and the excited states of common DSSC dyes. This energy alignment facilitates stepwise electron transfer, enhancing the efficiency of charge injection from the dye and improving carrier collection. For example, electrons may transfer from the dye to α-Fe_2O_3 and then to TiO_2, aided by graphene as a conductive channel. This tiered energy cascade promotes efficient charge separation and reduces charge loss during transport [31].

Suppression of charge recombination

Iron oxide nanoparticles can serve as barrier or blocking layers at the TiO_2/electrolyte interface. These barriers impede the back transfer of electrons from TiO_2 to the redox couple in the electrolyte, thus reducing charge recombination and improving open-circuit voltage (Voc) [30,31]. Their strategic placement within the porous TiO_2 framework ensures selective charge flow and protects sensitive electron pathways from recombination losses. Additionally, the surface of TiO_2 often contains defects and trap states that facilitate unwanted recombination. Iron oxide nanoparticles can passivate these surface traps, effectively reducing the number of recombination centers and increasing electron lifetimes. This passivation effect helps maintain a higher photocurrent and extends the operational stability of the DSSC [64,65]. While moderate Fe_2O_3 incorporation can enhance visible-light absorption and photocurrent, excessive iron content often introduces defect-mediated recombination centers, reducing open-circuit voltage and overall efficiency [66].

Synergistic Interactions within Iron Oxide-Graphene-TiO_2 Nanocomposites

The photoanode is an essential component in DSSCs which has great effect on the overall efficiency of the system. To achieve an efficient photoanode material, iron oxide and graphene can be incorporated into TiO_2 to form a composite material. When these materials interact together, they address some of the issues that confront TiO_2 photoanodes. Graphene plays an important role in improving electron mobility within the composite due to its exceptional conductivity and high surface area which helps to provide rapid electron transport channels and additional sites for dye adsorption to that of TiO_2 which is the main photoanode material [4,55]. Improved electron mobility reduces electron recombination by facilitating the faster extraction of photoexcited electrons from the dye through TiO_2 into the external circuit [14,55]. Ge *et al.* reported the fabrication of DSSC photoanodes by spin-coating graphene/TiO_2 composites with graphene loadings ranging from 0 to 10 wt.% onto indium tin oxide (ITO) substrates [26]. Compared with the pristine TiO_2 photoanode, which delivered a short-circuit current density (Jsc) of 188.3 A m^{-2} and a power conversion efficiency (PCE) of 5.98%, the photoanode containing 1 wt.% graphene exhibited a higher Jsc of 199.2 A m^{-2} and an improved PCE of 6.86%. This enhancement in Jsc was ascribed to more efficient charge collection, suppressed charge recombination, and increased dye adsorption resulting from the uniform dispersion of graphene within the TiO_2 matrix. In another study, Eshaghi and Aghaei investigated DSSCs based on graphene–TiO_2 composite photoanodes with varying graphene contents (0–2.0 wt.%). The results showed that dye adsorption increased with graphene loading due to the enhanced surface area and improved light-harvesting capability of the composites. The photovoltaic performance exhibited a strong dependence on graphene concentration, reaching an optimum at approximately 1.5 wt.%, where the power conversion efficiency (PCE) improved by approximately 42% compared with pristine TiO_2-based DSSCs [67]. This enhancement was attributed to improved electron transport and suppressed charge recombination, as graphene acted as a conductive bridge facilitating rapid electron extraction. However, further increases in graphene content led to a decline in efficiency due to light shielding effects and increased interfacial recombination, underscoring the

importance of precise graphene content optimization in composite DSSC photoanodes. Iron oxide (Fe_2O_3 or Fe_3O_4) also contributes to this system by extending the spectral response of the photoanode by narrowing the optical bandgap of the materials to enable it absorb more effectively from the E-M spectrum, thereby contributing to enhanced photon utilization [66–69]. In addition, iron oxide nanoparticles induce light scattering within the porous TiO_2 matrix, increasing the optical path length and boosting light harvesting. They also act as catalytic and electron-mediating centers, facilitating charge transfer at the TiO_2/electrolyte interface. For example, Kilic *et al*., reported that DSSCs fabricated with Fe_2O_3-modified TiO_2 photoanodes exhibited a power conversion efficiency of 7.27%, which is significantly higher than the 5.10% obtained for pristine anatase TiO_2 [31]. This notable enhancement in photovoltaic performance was attributed to improved light-harvesting capacity and a larger specific surface area, which facilitates increased dye adsorption in the Fe_2O_3-modified TiO_2 nanostructures. In another report, Chou *et al.* mentioned that DSSCs employing Fe_3O_4–TiO_2 composite photoelectrodes exhibit a higher short-circuit current density (Jsc) and an enhanced power conversion efficiency of 3.54%, compared to 2.35% for pristine TiO_2 [63]. This improvement is mainly attributed to the efficient Fe^{2+}/Fe^{3+} charge transfer, which provides additional electron transport pathways and suppresses recombination, as well as increased dye loading resulting from the enlarged surface area of the composite photoelectrode. The combination of iron oxide, graphene, and TiO_2 to form a nanocomposite results in strong synergistic interactions. Graphene compensates for the poor conductivity of iron oxide, ensuring efficient electron transport, while iron oxide enhances visible-light absorption and scattering, which TiO_2 alone cannot achieve [37,53,55]. TiO_2, in turn, provides the structural backbone for dye anchoring and stability. The synergistic interaction among these components improves dye loading, suppresses electron recombination, prolongs electron lifetime, and enhances overall charge collection efficiency. As a result, DSSCs fabricated with iron oxide–graphene–TiO_2 photoanodes typically have high potential to demonstrate higher short-circuit current density (Jsc), open-circuit voltage (Voc), and overall power conversion efficiency compared to conventional TiO_2-based devices [4,26,50].

Synthesis Methodologies for Iron Oxide-Graphene-TiO_2 Nanocomposites

The performance of nanocomposites used as photoanodes in DSSCs depends on the method of synthesis used in fabricating the material. The method of synthesis can influence the morphology, crystallinity, and surface properties of the resulting materials [67-70]. It also influences the charge transport behavior, light absorption efficiency, and interfacial contact within the composite. Table 3 presents a comparative overview of the various synthesis methods, highlighting their advantages, limitations, and relevance to DSSC performance. Over the years, numerous synthesis techniques have been developed for nanocomposite fabrication, including chemical co-precipitation, chemical vapor deposition, thermal decomposition, hydrothermal synthesis, solid-state reactions, and sol–gel methods.

Review on various methods of synthesis

Hydrothermal and solvothermal methods

Hydrothermal synthesis is one of the most commonly used methods for preparation of nanomaterials. It is basically a solution reaction-based approach. It refers to the synthesis by chemical reactions of substances in a sealed heated solution above the ambient temperature and pressure [71-73]. Among the various techniques employed for synthesizing Fe_2O_3-modified TiO_2, the hydrothermal method is particularly promising, as many conventional growth techniques require complex process control, and high processing temperatures [31]. In contrast, hydrothermal synthesis offers several advantages, including simple operation and precise control over particle size, morphology, size distribution, and crystallinity. These features can be effectively tuned by adjusting key reaction parameters such as temperature, reaction time, solvent and

surfactant type, and precursor composition, making the method highly versatile and suitable for scalable fabrication [72,73]. The solvothermal method is the hydrothermal process in the presence of a specific solvent. In this, organic solvents that have high boiling points can be selected, which enable the temperature to be raised much higher than in hydrothermal methods. The solvothermal method can be used to control the size, shape, and crystallinity of TiO_2 nanoparticles [48,74-76].

Chemical co-precipitation and co-deposition

The co-precipitation technique is becoming increasingly important for distributing materials and precursors used in a reaction to produce a required material. The aim of co-precipitation is to prepare multicomponent materials through the formation of intermediate precipitates, usually hydrous oxides or oxalates, so that an intimate mixture of components is formed during precipitation and chemical homogeneity is maintained upon calcination. In the typical process of co-precipitation, aqueous metal salts are mixed at sufficient temperatures with a base, which acts as a precipitating agent [77]. The advantage of the co-precipitation method is that it yields a crystalline size in a small range compared to other synthesis processes depending on the precipitating agent selected during the reaction. Additionally, the method is often preferred over other processes because it involves simple steps. The crystallite size and morphology of the material prepared using this method can be controlled through the use of capping agents. However, continuous washing, drying, and calcination to achieve a pure phase of phosphor are major disadvantages of the co-precipitation method [75,76].

Layer-by-layer assembly

Layer-by-layer (LbL) is simple and versatile strategy to prepare multifunctional nanomaterials; it was first proposed in 1966 by Iler who constructed multilayer assemblies via alternating adsorption of anionic and cationic colloidal particles. The fine regulation of the film thickness and structure provides an elegant way to tune the physical and chemical properties through mild assembly conditions (*e.g.,* pH and ion strength). The key competitive features of LbL are its mild aqueous assembly conditions, the absence of sophisticated and expensive equipment, the large freedom in selecting building materials, and the diverse driving forces for material assembly [42,77-79].

In situ growth and decoration techniques

The *in situ* growth and decoration technique is an effective approach for synthesizing iron oxide–graphene–TiO_2 nanocomposites with well-controlled morphology, intimate interfacial contact, and homogeneous dispersion of components. In this method, the nanoparticles (TiO_2 and Fe_2O_3) are directly nucleated and grown on the graphene surface during synthesis rather than being physically mixed after preparation. This ensures strong chemical bonding and uniform distribution, which minimizes particle aggregation and enhances electron transport pathways [80]. The decoration process in *in situ* methods refers to the controlled anchoring or deposition of iron oxide and TiO_2 nanoparticles on the graphene surface to achieve desired nanostructures—such as core–shell, layered, or network architectures. Decoration ensures intimate contact between the components, reducing charge-transfer resistance and promoting rapid electron mobility through the conductive graphene matrix. The *in situ* decorated Fe_2O_3 nanoparticles extend visible-light absorption, while TiO_2 maintains strong photocatalytic activity and structural stability. This synergy enhances the photoresponse and dye-sensitized solar cell (DSSC) performance, as electrons generated in Fe_2O_3 can efficiently migrate through graphene into TiO_2 and then to the external circuit. Additionally, in-situ decoration prevents the detachment of nanoparticles during device operation, improving long-term stability. Overall, this technique provides a scalable and environmentally friendly route for producing highly integrated ternary nanocomposites with superior optical, electrochemical, and photovoltaic properties.

Table 3: Comparison of various synthesis methods for iron oxide-graphene-TiO_2

Synthesis method	Process	Advantage	Limitation	Relevance to DSSCs performance	Ref.
Hydrothermal	Solution-based chemical reactions in sealed vessels at elevated temperature and pressure	Precise control over particle size, morphology, and crystallinity; high phase purity	Long reaction time; autoclave required; and limited scalability	High crystallinity enhances electron transport and reduces recombination in dssc photoanodes	[73]
Solvothermal	Hydrothermal process using high-boiling organic solvents	Higher reaction temperatures; improved control of size, shape, and crystallinity	Use of organic solvents; post-treatment required	Improved crystallinity and band structure tailoring enhance charge transport and light absorption	[74, 79]
Chemical co-precipitation / co-deposition	Simultaneous precipitation of metal precursors using a base to form mixed hydroxides/oxalates	Simple, low-cost; good compositional homogeneity; and small crystallite size	Repeated washing, drying, and calcination; possible agglomeration	Effective for iron oxide incorporation and bandgap tuning, leading to moderate dssc performance improvement	[72,75]
Layer-by-layer (LbL) assembly	Alternating adsorption of oppositely charged species to build multilayer films	Excellent control over film thickness, structure, and composition; mild aqueous conditions	Time-consuming; less suitable for bulk synthesis	Optimizes interfacial contact and charge transport, improving dssc efficiency and reproducibility	[79]
In-situ growth and decoration	Direct nucleation and growth of TiO_2 and Fe_2O_3 nanoparticles on graphene surfaces	Strong interfacial bonding; uniform dispersion; reduced aggregation; and enhanced stability	Requires precise process control	Superior electron transport, reduced charge-transfer resistance, extended visible-light absorption, and enhanced dssc efficiency	[80]

Impact of synthesis parameters on the morphology, composition, and interfacial properties of the nanocomposites

The morphology, phase composition, and interfacial architecture of iron oxide-graphene-TiO_2 nanocomposites are highly dependent on the synthesis parameters, including precursor concentration, solution pH, reaction temperature, annealing conditions, and the choice of reducing agents. These factors govern not only the particle size, crystallinity, and surface area of TiO_2 and iron oxide but also the dispersion and anchoring of nanoparticles on the graphene substrate. Variations in pH can influence nucleation kinetics and aggregation behavior, while annealing conditions dictate crystallographic phase transitions and interfacial bonding strength. Likewise, the type of reducing agent employed plays a crucial role

in modulating the reduction level of graphene oxide, thereby impacting its electrical conductivity and compatibility with the metal oxides. A fine-tuned balance of these synthesis conditions is therefore essential to achieve uniform dispersion, strong interconnectivity, and optimized charge transfer pathways, which are critical for enhancing the photoelectrochemical performance of DSSCs. In a study by Yudoyono *et al.* [81,82], it was reported that the pH value of solution during the co-precipitation synthesis of TiO_2 using $TiCl_3$ as a precursor has influence of the phase formed. It was reported (as presented in the Table 4) that at high pH (> 8), the phase of pure anatase was formed, and pure rutile phase was formed when the pH was adjusted < 5, while 5 < pH < 8 formed a mixed phase of anatase- brookite [82]. In another study by Tsega and Dejene, the effects of pH on the structural, morphological and optical properties of TiO_2 nanoparticles were investigated [83]. It was reported that at pH 4.4–6.8 only the anatase phase of TiO_2 is present while under strong acidic conditions at pH 3.2 rutile, brookite and anatase co-exist, but rutile is the predominant phase as shown by the XRD spectra in Figure 3. The figure presents a magnified view of the anatase (101) peak of TiO_2 at different pH values. A slight shift of the diffraction peak toward higher angles is observed with increasing hydrochloric acid concentration. This shift can be attributed to variations in lattice strain, including tensile and compressive strain, induced in the TiO_2 nanoparticles. The annealing temperature determines the crystallinity and the phase stability of TiO_2 and iron oxide (Fe_3O_4, γ-Fe_2O_3, or α-Fe_2O_3), which strongly influence electron transfer and light absorption. Chakraborty *et al.* reported that the synthesis of Fe_2O_3 nanoparticles via a chemical co-precipitation method followed by annealing at various temperatures ranging from 100 °C to 900 °C. The XRD analysis confirmed the synthesis of Fe_2O_3 NPs, with a phase transition from γ-Fe_2O_3 to α-Fe_2O_3 observed between 100 °C and 300 °C. Table 5 presents the effect of increase in annealing temperature on crystalline size of TiO_2. It was observed that the crystallite size increased with increase in annealing temperature, indicating enhanced crystallinity [84]. Furthermore, the degree of graphene reduction plays a dual role in determining the performance of iron oxide–graphene–TiO_2 nanocomposites. A higher reduction degree enhances the electrical conductivity of graphene, thereby facilitating faster electron transport and suppressing charge recombination. However, excessive reduction eliminates oxygen-containing functional groups (–OH, –COOH, and –C=O), which serve as active sites for nanoparticle nucleation and anchoring. Conversely, a partially reduced graphene structure maintains sufficient functional groups to promote strong interfacial bonding with TiO_2 and iron oxide, though at the expense of electrical conductivity. Therefore, optimizing the reduction degree is critical to achieving a balance between conductivity and interfacial compatibility, ensuring efficient electron transfer and structural stability in the composite [51]. Optimized parameters ensure a synergistic nanostructure with uniform dispersion, minimal recombination centers, and maximized interfacial contact for efficient charge separation.

Table 4: Phase of TiO_2 at different pH solution [82]

pH solution	Ratio of phase content (%)		
	Rutile	Anatase	Brookite
3	100	-	-
5	100	-	-
6	80	-	20
7	-	85	15
7,7	-	90	10
8	-	100	-
8,4	-	100	100

Table 5: Effect in the crystalline size of Fe_2O_3 at different annealing temperature [84]

Annealing temperature (°C)	Crystalline size (nm)	Structure
25	15.54	Inverse spinel
100	15.13	Inverse spinel
300	18.13	Rhombohedral
500	19.14	Rhombohedral
700	20.88	Rhombohedral
900	21.23	Rhombohedral

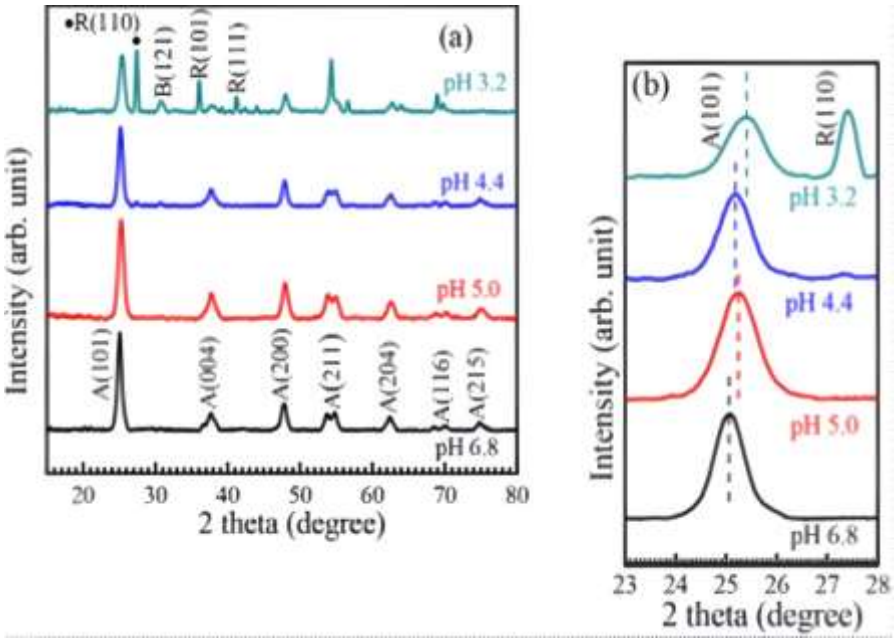

Figure 3: XRD pattern of TiO_2 at different pH solution [82]

Scalability and cost-effectiveness considerations for different synthesis routes

For the large-scale deployment of dye-sensitized solar cells (DSSCs), the choice of synthesis route must strike a careful balance between device performance, production scalability, and overall cost. Among the available methods, chemical co-precipitation is particularly attractive due to its low processing cost, simplicity, and suitability for bulk powder production, using inexpensive precursors and relatively mild reaction conditions [74]. The method is easily scalable to kilogram-level synthesis and is compatible with conventional slurry-based electrode fabrication techniques. However, its major limitations include limited control over crystallinity, particle size distribution, and interfacial defect density, which can adversely affect charge transport and recombination if not carefully optimized. In contrast, hydrothermal and solvothermal methods enable the growth of highly crystalline, uniform, and well-defined nanostructures, such as nanorods, nanotubes, and hierarchical architectures, which are beneficial for enhancing electron transport and dye loading [46]. Despite these advantages, these techniques typically require high-pressure autoclaves, elevated temperatures, and long reaction times, resulting in increased energy consumption and lower throughput. Such constraints limit their economic viability for mass production, particularly when large-area DSSC modules are considered [74]. Co-deposition methods allow direct fabrication of electrode films but require specialized instrumentation. From an industrial perspective, routes utilizing abundant precursors, room-temperature processes, and environmentally benign solvents are preferred.

Hybrid methods that combine low-cost co-precipitation with thin-film co-deposition may offer a pathway toward scalable, high-performance DSSCs.

Characterization Techniques and Performance Evaluation

Characterization methods are essential for understanding the relationships between synthesis, structure, properties, and performance of nanomaterials [77]. They provide direct insight into the structural, morphological, optical, chemical, and electrochemical features of materials, effectively bridging material design and functional performance in device applications [67,83]. Table 6 summarizes the various characterization techniques used to characterize iron oxide–graphene–TiO_2 nanocomposites.

Structural analysis (XRD, Raman Spectroscopy)

X-ray diffraction technique is a type of analytical technique that analyzes the crystalline phase, crystal structure, purity and average crystalline size of TiO_2 nanoparticles [61,83,84]. It is used for the examination of materials and thin films. XRD works on the principle of Bragg's equation, which is described in terms of reflection of collimated X-ray beam incident on a crystal plane of the sample that to be characterized. These X-rays are generated by a cathode ray tube, filtered to produce monochromatic radiation, collimated and directed towards the sample. To confirm the results obtained using XRD, microscopy techniques or other solid state characterization techniques can be compared with the results [85-87].

Raman spectroscopy provides information regarding the vibrational energy levels of molecules. Chemical structure, bonding, conformation, and intermolecular interactions between the molecules can be obtained from this technique [53,86]. Although it resembles IR spectroscopy, however the principle of Raman spectroscopy is based on inelastic light scattering. Raman spectroscopy is a valuable technique for the phase identification of nanomaterials. Raman spectroscopy provides insight into graphene quality (D and G bands), TiO_2 polymorphs, and iron oxide phases [88].

Morphological studies (SEM, TEM, AFM)

A scanning electron microscope (SEM) is a type of electron microscope that images a sample by scanning it with a high-energy beam of electrons in a raster scan pattern. The electrons interact with the atoms that make up the sample producing signals that contain information about the sample's surface topography, composition, and other properties such as electrical conductivity. SEM can produce very high-resolution images of a sample surface, revealing details about smaller than 1 to 5 nm in size. Due to the very narrow electron beam, SEM micrographs have a large depth of field, yielding a characteristic three-dimensional appearance useful for understanding the surface structure of a sample. SEM reveals surface texture, porosity, and film homogeneity [89]. Transmission electron microscopy is the method of analyzing particles in the range of nanometers. Here, a beam of electrons is passed through the sample to be analyzed. An image is formed by the interaction of the electrons with the sample being analyzed, which is magnified and then projected onto an imaging device. TEM shows nanoparticle size, distribution, and intimate graphene–oxide interfaces [53].

Also, surface texture is an important issue when the main interest is to understand the nature of material surfaces and it plays a significant role in the functional performance of many engineering components. On the ultramicroscopic scale of surfaces, atomic force microscopy (AFM) has been developed to obtain a three-dimensional image of a material surface on a molecular scale. AFM measures surface roughness, critical for dye loading efficiency. AFM has advantage of produing high-resolution images with a lateral resolution in the range of a few nanometers and vertical resolution less than 1 nm, it can be used to produce images from the surface of nonconductors (polymers) without any special preparation to make the sample conductive, as required in SEM and TEM, and it is well suited for characterization of nanocomposites.

Surface and chemical composition analysis (XPS and EDX)

X-ray photoelectron spectroscopy (XPS) is used to determine the quantitative elemental composition and oxidation state of materials, stoichiometry, electrical state and examine surface contamination [88,89]. EDX (Energy Dispersive X-ray Spectroscopy) provides elemental mapping, ensuring uniform dispersion of components. EDS detectors are typically integrated with SEM instruments to facilitate their combined use because the operational principle of EDS relies on electron beam excitation [90].

XPS is applicable for characterizing the surfaces of semiconductors, inorganic minerals, organic compounds, thin films and coated materials. Both XPS and energy dispersive X-ray spectroscopy (EDS) are used to detect the presence of elements in different materials [91,92]. However, the XPS provides information on the elemental composition of materials and differentiates the oxidation states of the elements, by taking measurements within a few atomic layers, usually from the top 1–10 nm of the surface [93]. The EDX method can determine the bulk composition of the elements with excitation volumes as deep as 3 μm deep into the sample [90].

Optical properties (UV-Vis spectroscopy)

Optical properties are fundamental characteristics that govern how materials interact with light, influencing their suitability for applications in photovoltaics, photocatalysis, optoelectronics, and sensors. Among various characterization techniques, Ultraviolet–Visible (UV-Vis) spectroscopy stands out as a versatile and non-destructive method to probe the light absorption behavior of materials in the 200–800 nm range [31]. It provides direct insights into electronic transitions, bandgap energies, charge-transfer dynamics, and light-harvesting efficiency, making it an indispensable tool in the study of nanomaterials. UV-Vis absorption spectra evaluate light harvesting, dye absorption, and bandgap modifications from Fe_xO_y incorporation.

Electrochemical behavior reported for Iron oxide–Graphene–TiO_2 photoanodes

CV is a widely employed technique to investigate the redox behavior, charge-transfer dynamics, and electrochemical stability of Fe_2O_3–TiO_2 nanocomposites. The incorporation of Fe_2O_3 into TiO_2 modifies the electronic structure by introducing additional redox-active centers, which can be observed in CV profiles as distinct anodic and cathodic peaks corresponding to Fe^{3+}/Fe^{2+} transitions. These redox couples enhance electron shuttling and facilitate improved interfacial charge transport between the electrode and electrolyte. In DSSC-related studies, Fe_2O_3-TiO_2 electrodes often show higher current densities in CV scans compared to bare TiO_2, reflecting enhanced electrocatalytic activity and reduced charge-transfer resistance [15].

Correlation of nanostructure properties with DSSC performance metrics (Jsc, Voc, FF, and η)

The structural and compositional features of iron oxide–TiO_2 composites play a crucial role in determining DSSC performance parameters. The short-circuit current density (Jsc) is improved through enhanced dye loading provided by the large surface area of graphene [4,92], along with additional light absorption contributed by iron oxide. The open-circuit voltage (Voc) is influenced by the suppression of charge recombination at the TiO_2/electrolyte interface, where Fe_xO_y can act as an effective blocking layer. Meanwhile, the fill factor (FF) benefits from the reduced charge transfer resistance enabled by the high electrical conductivity of graphene [27]. The synergistic interaction between the components brings about improvements in the overall efficiency. In 2022, Ahmad studied the effect of graphene material incorporated into the TiO_2 photoanode for DSSC application [94]. It was reported that the DSSC cell using the rGO composition photoanode exhibits greatly improved photovoltaic performance as compared to that of pure TiO_2.

Table 6: Summary of characterization techniques for iron oxide-graphene-TiO_2 photoanode material

Characterization method	Property analyzed	Relevance to DSSCs performance	Ref.
XRD	Structural / crystalline properties	Determines electron transport pathways and recombination behavior; anatase phase favors higher dssc efficiency	[91]
Raman spectroscopy	Structural and vibrational properties	Confirms composite formation and defect levels, which influence charge transfer and recombination	[50,53]
SEM	Surface morphology	Affects dye loading, electrolyte penetration, and interfacial contact	[53,87]
TEM	Microstructure	Confirms nanoscale heterojunctions that enhance charge separation and transport	[89]
AFM	Surface topography	Higher roughness improves dye adsorption and light harvesting	[31]
XPS	Surface chemistry	Verifies doping, chemical states, and interfacial charge-transfer capability	[93]
UV-Visible	Optical properties	Determines light absorption efficiency and bandgap tuning for enhanced photocurrent	[84]
Cyclic voltammetry	Electrochemical behavior	Indicates electrocatalytic activity and improved electron transport in DSSCS	[15]

rGO/TiO_2 with solution volume of 4 mL exhibited the best photovoltaic performance with the highest efficiency of 3.15% and the greatest current density of 5.98 mA/cm^2 (Table 7). This performance can be traced to the graphene material which improved the surface of TiO_2 for dye loading and also enhanced electron transport. Kılıç *et al.* [31] reported a significant enhancement of approximately 40% in solar conversion efficiency, incident photon-to-current efficiency (IPCE), and fill factor (FF) for Fe_2O_3-modified TiO_2 compared to bare TiO_2. Specifically, the Fe_2O_3–TiO_2-based DSSC achieved a power conversion efficiency of 7.27%, whereas the device with pure anatase TiO_2 showed an efficiency of 5.10%. This notable improvement in performance was attributed to enhanced light harvesting and the increased specific surface area of the Fe_2O_3-modified TiO_2 nanostructures, which facilitated greater dye adsorption [31].

Elucidating the mechanisms behind the observed performance enhancements through detailed analysis of characterization data

Performance gains can be traced back to synergistic mechanisms revealed by characterization XRD and Raman confirm crystalline phases responsible for charge transport and stability. Hatib [52] carried out an investigation on the performance enhancement of DSSC through TiO_2/rGO hybrid. He reported that analysis of the XRD test results on the DSSC crystal structure shows that the addition of rGO to TiO_2 affects the diffraction pattern and crystal structure formed. At a sintering temperature of 400 °C, the sharp diffraction peaks (Figure 4) indicate that the TiO_2 anatase structure reaches the highest degree of order. The shift and broadening of the diffraction peaks after adding rGO indicate a distortion in the TiO_2 crystal lattice, which increases the total surface area and electron transfer pathways.

Table 7: Comparison between photovoltaic parameter of DSSC with pure TiO_2 and rGO/TiO_2 [94]

Material	Solution volume (mL)	Voc (V)	Jsc (mA/cm²)	FF	Efficiency (η) %
TiO_2	1	0.752	0.605	47.625	0.206
	2	0.62	0.836	49.409	0.315
	3	0.795	1.116	48.412	0.430
	4	0.719	2.436	57.448	1.006
rGO/TiO_2	1	0.897	4.467	61.819	2.476
	2	0.892	4.53	62.564	2.531
	3	0.922	4.472	64.568	2.661
	4	0.906	5.983	58.117	3.151

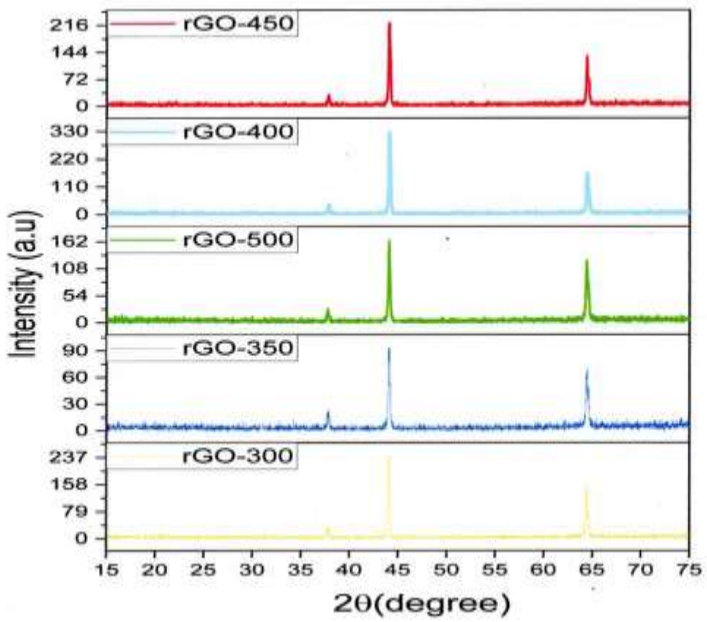

Figure 4: XRD test results for each heating variation [52]

It is observed here that thermal reduction promotes the removal of residual oxygen functional groups and facilitates the rearrangement of carbon atoms into more ordered sp^2 graphitic domains. This structural reorganization increases short-range order which leads to sharper and more intense XRD peaks, giving the appearance of improved crystallinity. The more regular crystal structure at the optimal sintering temperature of 400 °C is directly related to the highest efficiency achieved by DSSC, namely 0.1923% [52]. Pardhi *et al.* [15] examined the effect of adding 2% wt concentrations of Fe_2O_3 powder into TiO_2 thin films (Figure 5). The addition of 2 wt.% of Fe_2O_3 leads to reduction in crystallite size. It was interesting to examine the effect of adding different concentrations of synthesized Fe_2O_3 powder into TiO_2 thin films. The addition of 2 wt.% of Fe_2O_3 leads to reduction in crystallite size as presented in (Table 5). This mixing of Fe_2O_3 also increases the values of micro-strain together with the dislocation density which improves dye loading and light harvesting capacity of the material [15]. TEM/SEM demonstrates well-dispersed nanoparticles, correlating with high Jsc. Najafi *et al.* [95] examined the morphology of TiO_2 and graphene-WO_3-TiO_2 composite using scanning electron microscopy (SEM) images. In the image of pure TiO_2 (Figure 6a), the nanoparticles appear to be aggregated, which may affect the overall performance of the material.

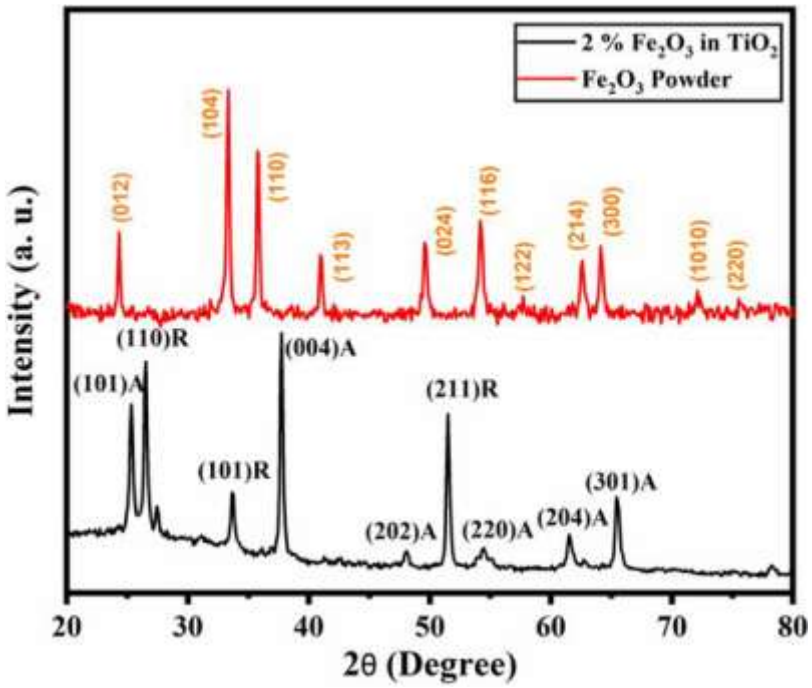

Figure 5: XRD pattern of Fe_2O_3 Powder, and 2 wt.% Fe_2O_3 in TiO_2 [15]

However, in the graphene-WO_3-TiO_2 composite (Figure 6b), it can be observed that TiO_2 nanoparticles are successfully deposited on the surface of 1D WO_3 nanorods, establishing a good interfacial contact between these two materials. This enhanced contact between WO_3 and TiO_2 can facilitate charge transfer during the photochemical reaction, which is beneficial for the overall performance of the composite [56]. AFM measures surface roughness, critical for dye loading efficiency. Ahmad et al., employed AFM to evaluate the surface roughness of TiO_2 thin films doped with different weight percentages of graphene oxide (GO) [58]. Figures 7a–7d present the three-dimensional surface morphologies of GO/TiO_2 thin films containing 0.0, 0.4, 0.6, and 0.8 wt.% GO, respectively. The average surface roughness increases progressively from 20.1 nm for pristine TiO_2 to 25.2, 35.1, and 39.3 nm for films with 0.4, 0.6, and 0.8 wt.% GO, respectively. This gradual increase in roughness suggests that GO incorporation enhances the surface area of the TiO_2 film, which is advantageous for dye adsorption and is therefore expected to improve light harvesting in DSSC photoanodes. XPS/EDX reveals chemical bonding and interfacial charge transfer, explaining reduced recombination and higher Voc. UV-Vis shows an extended absorption edge due to Fe_2O_3, aligning with enhanced light harvesting. The CV study reveals charge transfer kinetics and the electrochemical activities of nanomaterials. Collectively, these results provide a mechanistic understanding: graphene serves as a conductive bridge, iron oxides extend visible light absorption and passivate recombination sites, while TiO_2 provides structural stability and dye anchoring capacity leading to superior DSSC efficiency.

Challenges and Future Perspectives

Iron oxide–graphene–TiO_2 photoanodes face many challenges before they can be used widely in DSSCs. Finding the right composition is difficult. Too much graphene can block dye adsorption, while excessive iron oxide can create recombination centers. The morphology of TiO_2 also affects performance, as one-dimensional structures improve electron transport, while porous structures increase dye loading [26].

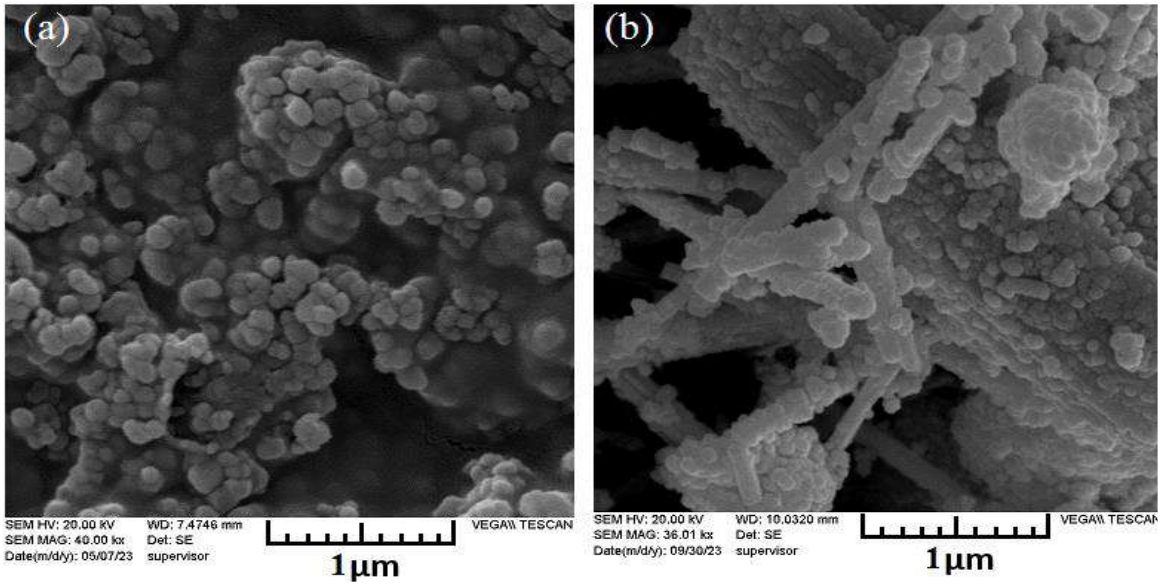

Figure 6: (a) SEM image of TiO_2 nanoparticle and (b) SEM image of graphene-WO_3-TiO_2 [56]

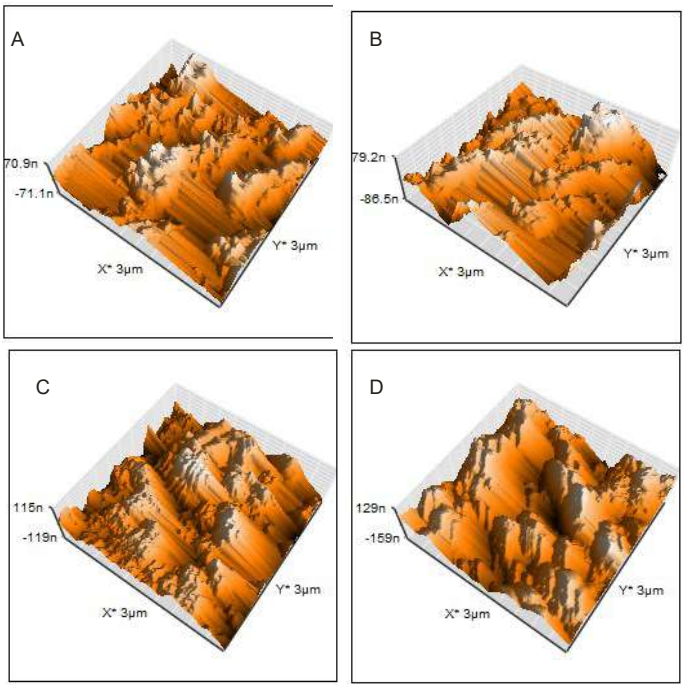

Figure 7: Topography AFM images of GO/TiO_2 film containing (a) 0.0 wt.%, (b) 0.4 wt.%, (c) 0.6 wt.%, and (d) 0.8 wt.% graphene oxide

Table 8: Crystalline size, micro-stain, and dislocation density of Fe_2O_3 powder and 2 wt.% Fe_2O_3 in TiO_2 [15]

Sample name	Crystalline size (D) (nm)	Micro-strain (ε) (10^{-4})	Dislocation De (δ) (10^{-4} nm^{-2}) density
Fe_2O_3 powder	80.58	15.51	1.54
2 wt.% Fe_2O_3 in TiO_2	74.51	19.62	1.8

Table 8 summarizes the XRD-derived crystalline size, micro-strain, and dislocation density of Fe_2O_3 powder and 2 wt.% Fe_2O_3-doped TiO_2. Another challenge is the limited understanding of how graphene, iron oxide, and TiO_2 interact. The exact role of energy band positions, charge carrier lifetimes, and graphene's oxidation state is unclear. Long-term stability is also a concern. Iron oxide can undergo photocorrosion, graphene may lose conductivity, and the electrode–electrolyte interface may degrade over time. In addition, current synthesis routes that yield high-quality nanostructures, such as hydrothermal and solvothermal methods, are too costly and energy-intensive for large-scale use [96]. Future work should focus on precisely tuning of composition and morphology to balance dye loading, charge transport, and recombination. Advanced tools such as time-resolved spectroscopy, theoretical modeling, and *in situ* electrochemical analysis can help explain the mechanisms at the interfaces. Stability can be improved through protective coatings, stronger anchoring strategies, and electrolyte engineering. For industrial use, cheaper and scalable methods such as chemical co-precipitation, spray pyrolysis, screen printing, and roll-to-roll deposition need to be developed. Novel device designs, including 3D hierarchical structures, tandem DSSCs, and flexible or transparent substrates, could further enhance efficiency and expand applications to wearable electronics or building-integrated photovoltaics. Combining Fe_2O_3, graphene, TiO_2 with other advanced materials and hybrid concepts also offers opportunities for future breakthroughs. With these efforts, laboratory progress can be translated into practical solar energy solutions.

Conclusion

This review highlights the important role of photoanode engineering in improving the efficiency and stability of DSSCs. Although TiO_2 remains the most established material due to its abundance, low cost, and environmental compatibility, its wide bandgap and relatively poor charge transport properties limit performance under visible light. To overcome these challenges, research has progressively focused on hybrid nanostructures that combine TiO_2 with complementary materials to enhance light absorption, electron mobility, and interfacial charge dynamics. Iron oxides and graphene are particularly attractive candidates when integrated with TiO_2. Fe_2O_3 introduces visible light activity and catalytic functionality, while graphene contributes outstanding conductivity and a high surface area that facilitates dye adsorption and electron transport. The synergistic effect of these components produces nanocomposites that address the shortcomings of pristine TiO_2, improving photon harvesting and reducing electron–hole recombination losses. The effectiveness of such composites, however, is highly dependent on synthesis conditions, which govern their morphology, crystallinity, and interfacial architecture. Characterization results from techniques such as XRD, CV, SEM, TEM, EDX and UV–Vis absorption reveal the benefits of optimized iron oxide–graphene–TiO_2 composites. Enhanced charge transfer, lower recombination resistance, and broader spectral absorption profiles confirm their potential for more efficient DSSCs. Therefore, the integration of iron oxide and graphene with TiO_2 represents a promising strategy for next-generation DSSC photoanodes.

ORCID

Kayode John Olaniyi
https://orcid.org/0009-0000-9998-5492
Sodiq Areo Akintoyese
https://orcid.org/0009-0008-8379-557X
Mayowa James Johnson
https://orcid.org/0009-0008-6214-4495
Joseph Olumide Ajiboye
https://orcid.org/0009-0007-9118-6435
Olufunke Lydia Adedeji
https://orcid.org/0000-0002-5982-8983
Gabriel Ayinde Alamu
https://orcid.org/0000-0003-2783-8738
Mojoyinola Kofoworola Awodele
https://orcid.org/0000-0002-6719-8328
Yekinni Kolawole Sanusi
https://orcid.org/0000-0001-6259-1166
Oluwaseun Adedokun
https://orcid.org/0000-0002-7947-8415

Reference

[1] Francis, O.I., Ikenna, A. Review of dye-sensitized solar cell (dsscs) development. *Natural Science*, **2021**, 13(12), 496-509.
[2] Karthick, S., Hemalatha, K., Balasingam, S.K., Manik Clinton, F., Akshaya, S., Kim, H.J. Dye-sensitized solar cells: History, components, configuration, and working principle. *Interfacial Engineering in Functional Materials for Dye-Sensitized Solar Cells*, **2019**, 1-16.
[3] Gu, D., Zhu, Y., Xu, Z., Wang, N., Zhang, C. Effects of ion doping on the optical properties of dye-sensitized solar cells. *Advances in Materials Physics and Chemistry*, **2014**, 4(10), 187-193.
[4] Muchuweni, E., Mombeshora, E.T., Muiva, C.M., Sathiaraj, T.S., Yildiz, A., Pugliese, D. Towards high-performance dye-sensitized solar cells by utilizing reduced graphene oxide-based composites as potential alternatives to conventional electrodes: A review. *Next Materials*, **2025**, 6, 100477.
[5] Lana, G.M., Bello, I.T., Adedokun, O.M., Adenigba, V.O., Jubu, P.R., Adedokun, O., Sanusi, Y.K., Dhlamini, M.S., Awodugba, A.O. One-dimensional TiO_2 nanocomposite-based photoanode for dye-sensitized solar cells: A review. *Solar Energy*, **2024**, 279, 112850.
[6] Malhotra, S.S., Ahmed, M., Gupta, M.K., Ansari, A., Metal-free and natural dye-sensitized solar cells: Recent advancements and future perspectives. *Sustainable Energy & Fuels*, **2024**, 8(18), 4127-4163.
[7] Yeoh, M.E., Chan, K.Y. Recent advances in photo-anode for dye-sensitized solar cells: A review. *International Journal of Energy Research*, **2017**, 41(15), 2446-2467.
[8] Sharma, K., Sharma, V., Sharma, S. Dye-sensitized solar cells: Fundamentals and current status. *Nanoscale research letters*, **2018**, 13(1), 381.
[9] Tamilselvan, S.N., Shanmugan, S. Towards sustainable solar cells: Unveiling the latest developments in bio-nano materials for enhanced dssc efficiency. *Clean Energy*, **2024**, 8(3), 238-257.
[10] Bhargava, C., Sharma, P.K. Use of natural dyes for the fabrication of dye-sensitized solar cell: A review. *Bulletin of the Polish Academy of Sciences. Technical Sciences*, **2021**, 69(6).
[11] Guo, X., Lu, G., Chen, J. Graphene-based materials for photoanodes in dye-sensitized solar cells. *Frontiers in Energy Research*, **2015**, 3, 50.
[12] Lü, X., Mou, X., Wu, J., Zhang, D., Zhang, L., Huang, F., Xu, F., Huang, S. Improved-performance dye-sensitized solar cells using Nb-doped TiO_2 electrodes: Efficient electron injection and transfer. *Advanced Functional Materials*, **2010**, 20(3), 509-515.
[13] Rahman, M.U., Wei, M., Xie, F., Khan, M., Efficient dye-sensitized solar cells composed of nanostructural ZnO doped with Ti. *Catalysts*, **2019**, 9(3), 273.
[14] Low, F.W., Lai, C.W. Recent developments of graphene-TiO_2 composite nanomaterials as efficient photoelectrodes in dye-sensitized solar cells: A review. *Renewable and Sustainable Energy Reviews*, **2018**, 82, 103-125.
[15] N. Pardhi, B. Prasad, P. K. Bhujbal, S. Jadkar, and H. M. Pathan, Deposition of Mixed Fe_2O_3 and TiO_2 Photoelectrode and their Application in Dye-Sensitized Solar Cells, *ES Chemistry and Sustainability,* **2025,** 4, 1655.
[16] Hasanuzzaman, M., Mokammel, M., Islam, M.J., Hashmi, S. Co-doped (N and Fe) TiO_2 photosensitising nanoparticles and their applications: A review. *Advances in Materials and Processing Technologies*, **2024**, 10(3), 1320-1343.
[17] Sharif, N.F.M., Kadir, M., Shafie, S., Rashid, S.A., Hasan, W.W., Shaban, S. Charge transport and electron recombination suppression in dye-sensitized solar cells using graphene quantum dots. *Results in Physics*, **2019**, 13, 102171.
[18] Adedokun, O., Titilope, K., Awodugba, A.O. Review on natural dye-sensitized solar cells (dsscs). *International Journal of Engineering Technologies IJET*, **2016**, 2(2), 34-41.
[19] Saud, P.S., Bist, A., Kim, A.A., Yousef, A., Abutaleb, A., Park, M., Park, S.J., Pant, B. Dye-sensitized solar cells: Fundamentals, recent progress, and optoelectrical properties improvement strategies. *Optical Materials*, **2024**, 150, 115242.
[20] Shittu, H., Bello, I., Kareem, M., Awodele, M., Sanusi, Y., Adedokun, O. Recent developments on the

photoanodes employed in dye-sensitized solar cell. *IOP Conference Series: Materials Science and Engineering*, **2020**, 805(1), 012019.
[21] Lau, S.C.T., Dayou, J., Sipaut, C.S., Mansa, R.F. Development in photoanode materıals for highly efficient dye sensitized solar cells. *International Journal of Renewable Energy Research*, **2014**, 4(3), 665-674.
[22] Alkuam, E. Preparation of multi-wall carbon nanotubes/graphene composites with cadmium sulfide in dye-sensitized solar cells (DSSCS). *Advances in Materials Physics and Chemistry*, **2021**, 11(6), 111-119.
[23] Zulkapli, M., Rashid, N., Sokri, M.N.M., Nasri, N. Study on optical properties of graphene-TiO_2 nanocomposite as photoanodes layer in dye sensitized solar cell (dssc). *Environment & Ecosystem Science (EES)*, **2018**, 2, 39-41.
[24] Derbali, S., Tiouitchi, G., Mounkachi, O., Almaggoussi, A., Moudam, O., Hybrid 2D phosphorene-black carbon material for dye-sensitized solar cells as counterelectrode. *Advanced Energy and Sustainability Research*, **2025**, 6(1), 2400197.
[25] Effendi, N., Samsi, N., Zawawi, S., Hassan, O., Zakaria, R., Yahya, M., Ali, A. Studies on graphene zinc-oxide nanocomposites photoanodes for high-efficient dye-sensitized solar cells. *AIP Conference Proceedings*, **2017**, 1877(1), 090005.
[26] Ge, C., Rahman, M.M., Nath, N.C.D., Ju, M.J., Noh, K.M., Lee, J.J. Graphene-incorporated photoelectrodes for dye-sensitized solar cells#. *Bulletin of the Korean Chemical Society*, **2015**, 36(3), 762-771.
[27] Makal, P., Das, D. Reduced graphene oxide-laminated one-dimensional TiO_2–bronze nanowire composite: An efficient photoanode material for dye-sensitized solar cells. *ACS Omega*, **2021**, 6(6), 4362-4373.
[28] Acik, M., Chabal, Y.J. A review on reducing graphene oxide for band gap engineering. *Journal of Materials Science Research*, **2012**, 2(1).
[29] Hamid, A.M., Hassan, H.W., Osman, F.A., Enhancement of solar cell efficiency by using TiO_2 nanostructure doped Fe_2O_3 dye and effect concentration of solvent on optical properties. *Asian Journal of Physical and Chemical Sciences*, **2019**, 7(3), 1-14.
[30] Im, J.S., Lee, S.K., Lee, Y.S. Cocktail effect of Fe_2O_3 and TiO_2 semiconductors for a high-performance dye-sensitized solar cell. *Applied Surface Science*, **2011**, 257(6), 2164-2169.
[31] Kılıç, B., Gedik, N., Mucur, S.P., Hergul, A.S., Gür, E. Band gap engineering and modifying surface of TiO_2 nanostructures by Fe_2O_3 for enhanced-performance of dye sensitized solar cell. *Materials Science in Semiconductor Processing*, **2015**, 31, 363-371.
[32] Shukla, B.K., Rawat, S., Gautam, M.K., Bhandari, H., Garg, S., Singh, J. Photocatalytic degradation of orange g dye by using bismuth molybdate: Photocatalysis optimization and modeling via definitive screening designs. *Molecules*, **2022**, 27(7), 2309.
[33] Jain, B., Gade, J.V., Hadap, A., Ali, H., Katubi, K.M., Sasikumar, B., Rawat, R. A facile synthesis and properties of graphene oxide-titanium dioxide-iron oxide as fenton catalyst. *Adsorption Science & Technology*, **2022**, 2022, 2598536.
[34] Mehralipour, J., Bagheri, S., Gholami, M., Synthesis and characterization of rGO/Fe0/Fe_3O_4/TiO_2 nanocomposite and application of photocatalytic process in the decomposition of penicillin G from aqueous. *Heliyon*, **2023**, 9(7).
[35] Awsha, A., Alazoumi, S., Elhub, B., A review on the development of TiO_2 photoanode for solar applications. *Albahit J Appl Sci*, **2021**, 2(2), 9-16.
[36] Makal, P., Das, D. Reduced graphene oxide-laminated one-dimensional TiO_2–bronze nanowire composite: An efficient photoanode material for dye-sensitized solar cells. *ACS Omega*, **2021**, 6(6), 4362-4373.
[37] Batmunkh, M., Dadkhah, M., Shearer, C.J., Biggs, M.J., Shapter, J.G. Incorporation of graphene into SnO_2 photoanodes for dye-sensitized solar cells. *Applied Surface Science*, **2016**, 387, 690-697.
[38] Calogero, G., Calandra, P., Irrera, A., Sinopoli, A., Citro, I., Di Marco, G. A new type of transparent and low cost counter-electrode based on platinum nanoparticles for dye-sensitized solar cells. *Energy & Environmental Science*, **2011**, 4, 1838-1844.
[39] Sivakumar, A., Shahid, M., Muthukumar, S., Balaji, A. DeepTracking from Aerial Platforms. *Asian Conference on Innovation in Technology (ASIANCON)*, **2021.**
[40] Mironyuk, I., Soltys, L., Tatarchuk, T., Savka, K.O. Methods of titanium dioxide synthesis. *Physics and Chemistry of Solid State*, **2020**, 21(3), 462-477.
[41] Vandebriel, R.J., Vermeulen, J.P., van Engelen, L.B., de Jong, B., Verhagen, L.M., de la Fonteyne-Blankestijn, L.J., Hoonakker, M.E., de Jong, W.H. The crystal structure of titanium dioxide nanoparticles influences immune activity in vitro and in vivo. *Particle and Fibre Toxicology*, **2018**, 15(1), 9.
[42] Zhang, C., Wu, Q., Ke, X., Wang, J., Jin, X., Xue, S. Ultrathin hematite films deposited layer-by-layer on a TiO_2 underlayer for efficient water splitting under visible light. *International Journal of Hydrogen Energy*, **2014**, 39(27), 14604-14612.
[43] Hu, Z., Lin, Z., Su, J., Zhang, J., Chang, J., Hao, Y. A review on energy band-gap engineering for

perovskite photovoltaics. *Solar Rrl*, **2019**, 3(12), 1900304.
[44] Cavallo, C., Di Pascasio, F., Latini, A., Bonomo, M., Dini, D. Nanostructured semiconductor materials for dye-sensitized solar cells. *Journal of Nanomaterials*, **2017**, 2017(1), 5323164.
[45] Bello, I.T., Oladipo, A.O., Adedokun, O., Dhlamini, S.M. Recent advances on the preparation and electrochemical analysis of mos2-based materials for supercapacitor applications: A mini-review. *Materials Today Communications*, **2020**, 25, 101664.
[46] Ali, I., Suhail, M., Alothman, Z.A., Alwarthan, A. Recent advances in syntheses, properties and applications of TiO_2 nanostructures. *RSC Adv.*, **2018**, 8, 30125-30147.
[47] Raza, G. Titanium dioxide nanomaterials, synthesis, stability and mobility in natural and synthetic porous media. **2017**.
[48] Kumar, A., Pandey, G. Different methods used for the synthesis of TiO_2 based nanomaterials: A review. *Am. J. Nano Res. Appl*, **2018**, 6(1), 1-10.
[49] Scarpelli, F., Mastropietro, T.F., Poerio, T., Godbert, N. Mesoporous TiO_2 thin films: State of the art. *Titanium Dioxide-Material for a Sustainable Environment*, **2018**, 508(1), 135-142.
[50] Ghayoor, R., Keshavarz, A., Rad, M.N.S., Mashreghi, A. Enhancement of photovoltaic performance of dye-sensitized solar cells based on TiO_2-graphene quantum dots photoanode. *Materials Research Express*, **2018**, 6(2), 025505.
[51] Wei, L., Chen, S., Yang, Y., Dong, Y., Song, W., Fan, R. Reduced graphene oxide modified TiO_2 semiconductor materials for dye-sensitized solar cells. *RSC Advances*, **2016**, 6(103), 100866-100875.
[52] Hatib, R., Anwar, K., Magga, R., Astak, M.A., Widhiyanuriyawan, D., Wardoyo, W. Performance enhancement of dye sensitized solar cell (dssc) through TiO_2/rGO hybrid: Comprehensive study on synthesis and characterization. *Journal of Mechanical Engineering Science and Technology (JMEST)*, **2024**, 8(1), 11.
[53] Khannam, M., Sharma, S., Dolui, S., Dolui, S.K. A graphene oxide incorporated TiO_2 photoanode for high efficiency quasi solid-state dye sensitized solar cells based on a poly-vinyl alcohol gel electrolyte. *RSC Advances*, **2016**, 6(60), 55406-55414.
[54] Korir, B.K., Kibet, J.K., Ngari, S.M., A review on the current status of dye-sensitized solar cells: Toward sustainable energy. *Energy Science & Engineering*, **2024**, 12(8), 3188-3226.
[55] Kusumawati, Y., Martoprawiro, M., Pauporté, T. Effects of graphene in graphene/ TiO_2 composite films applied to solar cell photoelectrode. *The Journal of Physical Chemistry C*, **2014**, 118(19), 9974-9981.
[56] Gilani, N., Fallahdoost Moghadam, S., Yousefi, A. Investigating the performance of the graphene-WO3-TiO_2 ternary composite in dye-sensitized solar cells. *Iranian Journal of Chemical Engineering (IJChE)*, **2024**, 20(4), 13-26.
[57] Mustafa, M.N., Sulaiman, Y. Fully flexible dye-sensitized solar cells photoanode modified with titanium dioxide-graphene quantum dot light scattering layer. *Solar Energy*, **2020**, 212, 332-338.
[58] Fotoelektrod, T.D.S. Performance enhancement of dye sensitized solar cell using graphene oxide doped titanium dioxide photoelectrode. *Malaysian J Anal Sci*, **2017**, 21, 928-940.
[59] Wei, L., Wang, P., Yang, Y., Dong, Y., Fan, R., Song, W., Qiu, Y., Yang, Y., Luan, T. Enhanced performance of dye sensitized solar cells by using a reduced graphene oxide/ TiO_2 blocking layer in the photoanode. *Thin Solid Films*, **2017**, 639, 12-21.
[60] Singh, A., Saini, Y.K., Kumar, A., Gautam, S., Kumar, D., Dutta, V., Lee, H.K., Lee, J., Swami, S.K. Property modulation of graphene oxide incorporated with TiO_2 for dye-sensitized solar cells. *ACS Omega*, **2022**, 7(48), 44170-44179.
[61] Eom, T.S., Kim, K.H., Bark, C.W., Choi, H.W. Influence of Fe_2O_3 doping on TiO_2 electrode for enhancement photovoltaic efficiency of dye-sensitized solar cells. *Molecular Crystals and Liquid Crystals*, **2014**, 600(1), 39-46.
[62] Rheima, A., Abdulah, H., Hussain, D., Abed, H., Abbas, Z. Synthesis of α-Fe_2O_3 nanoparticles by photolysis method for novel dye-sensitized solar cell. *Journal Advanced Sciences and Nanotechnology*, **2022**, 1, 1-8.
[63] Chou, J.C., Chu, C.M., Liao, Y.H., Lai, C.H., Lin, Y.J., You, P.H., Hsu, W.Y., Lu, C.C., Nien, Y.H. An investigation on the photovoltaic properties of dye-sensitized solar cells based on Fe_3O_4–TiO_2 composited photoelectrode. *IEEE Journal of the Electron Devices Society*, **2016**, 5(1), 32-39.
[64] Kodan, N., Agarwal, K., Mehta, B., All-oxide α-Fe_3O_4/h: TiO_2 heterojunction photoanode: A platform for stable and enhanced photoelectrochemical performance through favorable band edge alignment. *The Journal of Physical Chemistry C*, **2019**, 123(6), 3326-3335.
[65] Li, F., Jian, J., Wang, S., Zhang, Z., Jia, L., Guan, X., Xu, Y., Wang, H. Tio_2 passivation layers with laser derived pn heterojunctions enable boosted photoelectrochemical performance of α- Fe_2O_3 photoanodes. *Chemical Engineering Journal*, **2023**, 461, 141872.
[66] Srivastava, A., Satrughna, J.A.K., Tiwari, M.K., Kanwade, A., Yadav, S.C., Bala, K., Shirage, P.M. Effect of Ti_1–$xFexO_2$ photoanodes on the performance of dye-sensitized solar cells utilizing natural betalain pigments extracted from Beta vulgaris (BV). *Energy Advances*, **2023**, 2(1), 148-160.

[67] Eshaghi, A., Aghaei, A.A. Effect of TiO_2–graphene nanocomposite photoanode on dye-sensitized solar cell performance. *Bulletin of Materials Science*, **2015**, 38(5), 1177-1182.
[68] Kodan, N., Agarwal, K., Mehta, B. All-oxide α-Fe_2O_3/h: TiO_2 heterojunction photoanode: A platform for stable and enhanced photoelectrochemical performance through favorable band edge alignment. *The Journal of Physical Chemistry C*, **2019**, 123(6), 3326-3335.
[69] Oseghe, E.O., Ndungu, P.G., Jonnalagadda, S.B. Synthesis, characterization, and application of TiO_2 nanoparticles–effect of ph adjusted solvent. *Journal of Advanced Oxidation Technologies*, **2015**, 18(2), 253-263.
[70] Singh, A.P., Kodan, N., Mehta, B.R., Held, A., Mayrhofer, L., Moseler, M. Band edge engineering in $BiVO_4$/ TiO_2 heterostructure: Enhanced photoelectrochemical performance through improved charge transfer. *ACS Catalysis*, **2016**, 6(8), 5311-5318.
[71] Miao, C., Shi, T., Xu, G., Ji, S., Ye, C. Photocurrent enhancement for Ti-doped Fe_2O_3 thin film photoanodes by an in situ solid-state reaction method. *ACS APPLIED Materials & Interfaces*, **2013**, 5(4), 1310-1316.
[72] Zhao, H., Fu, W., Yang, H., Xu, Y., Zhao, W., Zhang, Y., Chen, H., Jing, Q., Qi, X., Cao, J. Synthesis and characterization of TiO_2/ Fe_2O_3 core–shell nanocomposition film and their photoelectrochemical property. *Applied Surface Science*, **2011**, 257(21), 8778-8783.
[73] Gan, Y.X., Jayatissa, A.H., Yu, Z., Chen, X., Li, M. Hydrothermal synthesis of nanomaterials. *Journal of Nanomaterials*, **2020**, 2020.
[74] Rane, A.V., Kanny, K., Abitha, V.K., Thomas, S. Methods for synthesis of nanoparticles and fabrication of nanocomposites. *Synthesis of Inorganic Nanomaterials*, **2018**, 121-139.
[75] Ba-Abbad, M.M., Benamour, A., Ewis, D., Mohammad, A.W., Mahmoudi, E. Synthesis of Fe_3O_4 nanoparticles with different shapes through a co-precipitation method and their application. *Jom*, **2022**, 74(9), 3531-3539.
[76] Vijayalakshmi, R., Rajendran, V. Synthesis and characterization of nano-TiO_2 via different methods. *Arch. Appl. Sci. Res*, **2012**, 4(2), 1183-1190.
[77] Bajaj, N., Joshi, R. Energy materials: Synthesis and characterization techniques. *Energy Materials*, **2021**, 61-82.
[78] Bellardita, M., Di Paola, A., Yurdakal, S., Palmisano, L. Preparation of catalysts and photocatalysts used for similar processes. *Heterogeneous Photocatalysis*, **2019**, 25-56.
[79] Zhang, S., Xia, F., Demoustier-Champagne, S., Jonas, A.M. Layer-by-layer assembly in nanochannels: Assembly mechanism and applications. *Nanoscale*, **2021**, 13(16), 7471-7497.
[80] Wang, K., Liu, B., Li, J., Liu, X., Zhou, Y., Zhang, X., Bi, X., Jiang, X. In-situ synthesis of TiO_2 nanostructures on Ti foil for enhanced and stable photocatalytic performance. *Journal of Materials Science & Technology*, **2019**, 35(4), 615-622.
[81] Sahadevan, J., Sojiya, R., Padmanathan, N., Kulathuraan, K., Shalini, M., Sivaprakash, P., Muthu, S.E. Magnetic property of Fe_2O_3 and Fe_3O_4 nanoparticle prepared by solvothermal process. *Materials Today: Proceedings*, **2022**, 58, 895-897.
[82] Yudoyono, G., Zharvan, V., Ichzan, N., Daniyati, R., Indarto, B., Pramono, Y.H., Zainuri, M., Darminto. Influence of ph on the formulation of TiO_2 powder prepared by co-precipitation of $TiCl_3$ and photocatalytic activity. *AIP Conference Proceedings*, **2016**, 1710(1), 030011.
[83] Tsega, M., Dejene, F. Influence of acidic ph on the formulation of TiO_2 nanocrystalline powders with enhanced photoluminescence property. *Heliyon*, **2017**, 3(2).
[84] Chakraborty, A.R., Toma, F.T.Z., Alam, K., Yousuf, S.B., Hossain, K.S. Influence of annealing temperature on Fe_2O_3 nanoparticles: Synthesis optimization and structural, optical, morphological, and magnetic properties characterization for advanced technological applications. *Heliyon*, **2024**, 10(21).
[85] Wang, Y., Li, Z., He, Y., Li, F., Liu, X., Yang, J. Low-temperature solvothermal synthesis of graphene–TiO_2 nanocomposite and its photocatalytic activity for dye degradation. *Materials Letters*, **2014**, 134, 115-118.
[86] Mallick, P., Dash, B. X-ray diffraction and uv-visible characterizations of α- Fe_2O_3 nanoparticles annealed at different temperature. *Nanosci. Nanotechnol*, **2013**, 3(5), 130-134.
[87] Cheng, H.H., Chen, S.S., Yang, S.Y., Liu, H.M., Lin, K.S. Sol-gel hydrothermal synthesis and visible light photocatalytic degradation performance of Fe/N codoped TiO_2 catalysts. *Materials*, **2018**, 11(6), 939.
[88] Nandee, R., Chowdhury, M.A., Hossain, N., Rana, M.M., Mobarak, M.H., Islam, M.A., Aoyon, H. Experimental characterization of defect-induced raman spectroscopy in graphene with bn, ZnO, Al_2O_3, and TiO_2 dopants. *Results in Engineering*, **2024**, 21, 101738.
[89] Sharma, V. A review on characterization of solid dispersion. *International Journal of Engineering Appl. Sci. Technol*, **2019**, 4, 127-128.
[90] Jacob, G., Min, H. A brief overview of x-ray photoelectron spectroscopy characterization of thin films. *Res. J. Chem. Environ*, **2024**, 28, 142-160.
[91] Solís-Casados, D.A., Escobar-Alarcón, L., Alvarado-Pérez, V., Haro-Poniatowski, E. Photocatalytic activity under simulated sunlight of bi-

modified TiO_2 thin films obtained by sol gel. *International Journal of Photoenergy*, **2018**, 2018(1), 8715987.
[92] Li, L., Mao, L., Yang, J. A review of principles, analytical methods, and applications of sem-eds in cementitious materials characterization. *Advanced Materials Technologies*, **2025**, 10(7), 2401175.
[93] Maximov, M., Nazarov, D., Rumyantsev, A., Koshtyal, Y., Ezhov, I., Mitrofanov, I., Kim, A., Medvedev, O., Popovich, A. Atomic layer deposition of lithium–nickel–silicon oxide cathode material for thin-film lithium-ion batteries. *Energies*, **2020**, 13(9), 2345.
[94] Ahmad, N., Talib, A. Effect of graphene material combined into titanium dioxide in dye-sensitized solar cells application. *Proceedings: Liga Ilmu Serantau*, **2022**, 8(1), 51-56.
[95] Najafi, M., Kermanpur, A., Rahimipour, M.R., Najafizadeh, A. Effect of TiO_2 morphology on structure of TiO_2-graphene oxide nanocomposite synthesized via a one-step hydrothermal method. *Journal of Alloys and Compounds*, **2017**, 722, 272-277.
[96] Le, T.L.T., Le, T.H.T., Van, K.N., Van Bui, H., Le, T.G., Vo, V. Controlled growth of TiO_2 nanoparticles on graphene by hydrothermal method for visible-light photocatalysis. *Journal of Science: Advanced Materials and Devices*, **2021**, 6(4), 516-527.